Science Press

ARTICLE

Spall of Al7050 Alloy with Different Thicknesses Under Ultrahigh Strain Rate Laser Shock Peening

Wu Junfeng,   Zou Shikun,   Che Zhigang,   Gong Shuili,   Cao Ziwen

Science and Technology on Power Beam Processes Laboratory, AVIC Manufacturing Technology Institute, Beijing 100024, China

Abstract: The spall characteristics of Al7050 alloy with different thicknesses treated by laser shock peening (LSP) with different process parameters (Process-1 and Process-2) were investigated to obtain the spall mechanism and spall threshold. The particle velocity of rear free surface and spall crater morphology in 0.33 mm thick Al7050 induced by LSP with Process-1 were measured and analyzed by a Photonic Doppler Velocimetry (PDV) system and scanning electron microscope (SEM), respectively. Spall sizes, spall thicknesses and spall fracture morphology in 5 mm thick Al7050 induced by LSP with Process-2 were analyzed by C-scan ultrasonic nondestructive testing with water immersion, optical microscope (OM) and SEM, respectively. The spall strength and LSP strain rate of 0.33 mm thick Al7050 were calculated by PDV data. Spall crater morphology was also analyzed. Results show that the spall sizes of 5 mm thick Al7050 increase with continued multiple LSP impacts and its spall thicknesses are in the range from 343 μm to 364 μm. Spall mechanism is mixture ruptures of ductile behavior with spherical voids and brittle behavior with straight cracks. Continued LSP-5 was the spall threshold of 5 mm thick Al7050. Compared with as-received material, the micro-hardness of 5 mm thick Al7050 with continued LSP-5 increases in the surface layer and decreases near rear free surface. The results provide not only some important insights on the spall behavior of aluminum alloy with laser shock but also fundamental research for avoiding the spall in industrial applications.

Key words: Al7050 alloy; laser shock peening; spall mechanism; spall threshold; spall fracture morphology

Laser shock peening (LSP) is a novel surface treatment technology, which has been widely used to improve fatigue life[1] and foreign object damage resistance of blades[2]. During LSP process, metal surface is irradiated with a laser beam of high energy intensity (GW/cm^2) and short pulse widths (ns). Then laser shock wave with high pressure (GPa) and high strain rate ($10^6 \, s^{-1}$) is generated due to the volume expansion of plasma and its blast[3], which spreads into the metals. When the peak pressure of laser shock wave exceeds Hugoniot elastic limit (HEL) of metals, severe plastic deformation and surface modification are obtained in the surface layer of metals. LSP introduces compressive residual stress layer with about 1 mm depth, refined grains and low surface roughness[4]. However, there are some problems at the edge of blades with LSP, such as bending deformations[5], and the internal damage induced by dynamic tensile stress[6], especially the spall. The

spall would rapidly decrease the fatigue life of components.

The spall induced by certain dynamic tensile stress, generated by the interaction between the incident unloading wave and the reflected release wave, is a kind of internal rupture[7-9]. Some researchers have investigated the spall strength of pure aluminum with LSP. Tollier et al[10] and Wang et al[11] found that the spall strength of pure aluminum rapidly increased with LSP strain rate more than $10^6 \, s^{-1}$. Wang et al[12] reported the effect of aluminum microstructures on the spall strength by a series of plate impact spall experiments. Resseguier et al[13] studied the spall strength of 500-μm-thick aluminum, which was impacted by 250-μm-thick aluminum flyers. However, the spall strength and LSP strain rates of Al7050 alloy were seldom reported.

In addition, more attentions had been paid to spall thickness and spall mechanism of metals with LSP. Cottet et al[14]

studied the spall thickness of aluminum with different thicknesses treated by LSP with laser power density (TW/cm²). The results indicated that 35-μm-thick spall, 100-μm-thick spall and 140-μm-thick spall were generated in 200-μm-thick aluminum with pulse width of 0.6 ns, 1000-μm-thick aluminum with pulse width of 2 ns and 900-μm-thick aluminum with pulse width of 35 ns, respectively. Tyler et al[15] reported the spall mechanism of Ti64 with 6-mm and 12-mm thicknesses treated by plate impact experiments. The spall micro-mechanism was nucleation, propagation and coalescence of micro-voids. However, the spall thickness and spall mechanism of Al7050 with 5 mm thickness treated by LSP were seldom investigated.

Furthermore, the research of spall fracture morphology would further explore the potential correlations between microscopic structures and the continuum spall. Lescoute et al[16] investigated the spall fracture morphology of 200-μm-thick aluminum with high energy laser irradiation of TW/cm². Rességuier et al[17] investigated the facture morphology in the spall craters of 260 μm thick tin foils treated by LSP with laser energy of 22~990 J, pulse duration of 3~5 ns and spot size of Φ2~Φ4 mm. Jarmakani et al[18] reported the spall fracture morphologies of polycrystal and monocrystal with LSP. Wielewski et al[19] showed the nature of spall initiation and propagation in TC4 with plate impact experiments. The spall initiation was the nucleation of voids at the grain boundaries between plastically hard/soft grains of the dominant hcp *α* phase. The spall propagation was the growth/coalescence of the nucleated voids. Dalton et al[20] investigated that the spall fracture morphologies of Al alloy with refined grains were a combination of brittle intragranular fracture and ductile transgranular fracture. However, it was seldom studied that the spall fracture morphology of 5-mm-thick Al7050 treated by LSP (GW/cm²).

In the present paper, the spall characteristics of Al7050 with different thicknesses were analyzed. The LSP strain rate, spall strength, spall size and spall thickness of Al7050 were measured and formulated. Moreover, the spall fracture morphologies and its whole cross-sectional micro-hardness were also observed. These topics discussed could provide some important insights on the spall behavior of aluminum alloy, which would be beneficial to LSP application in industry.

1 Experiment

Al7050 with the dimensions of 50 mm×50 mm×5 mm and Φ20 mm×0.33 mm were selected as experiment material. The chemical composition (wt%) is listed in Table 1. The mechanical properties were elastic modulus of 72 GPa, Poisson's ratio of 0.33 and HEL of 1.1 GPa. The surface of Al7050 was treated by continued multiple LSP impacts at single spot (LSP-1~LSP-8) by Nd:YAG laser system, as shown in Fig.1. The pulse frequency was 1 Hz and laser wavelength was 1064 nm. The LSP process parameters are labeled as Process-1 and Process-2, as listed in Table 2. The Al7050 with 0.33 mm thickness and 5 mm thickness were treated by Process-1 and Process-2, respectively.

The rear free surface velocity of 0.33 mm thick Al7050 was measured by a photonic Doppler velocimetry (PDV) system to obtain the spall strength and LSP strain rate[21]. The fracture morphology of the spall crater of 0.33 mm thickness Al7050 was analyzed by scanning electron microscope (SEM) with SUPRA55.

5 mm thick Al7050 was measured by a C-scan ultrasonic nondestructive testing with water immersion to analyze the plane spall sizes. C-scan ultrasonic nondestructive testing apparatus includes KSI ultrasonic microscopic detection system and ultrasonic longitudinal wave vertical reflection method. Instrument parameters were 50 MHz focusing probe with water immersion, 0.8~24 dB sensitivity, and scan imaging ×500 (0.1 mm scan spacing). The cross-sectional spall thickness and spall fracture characteristics of 5 mm thick Al7050 were analyzed by optical microscope (OM) and SEM. The corrosive liquid was hydrofluoric:nitric acid:water=1:2:7

Table 1 Chemical composition of Al7050 (wt%)

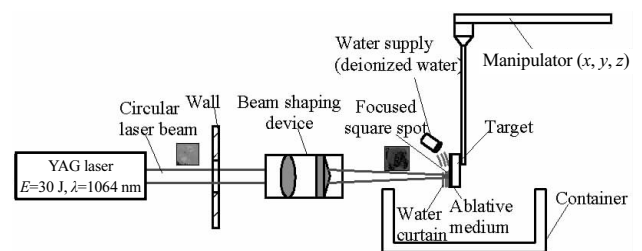| Zn	Mg	Cu	Cr	Zr	Si	Fe	Al
5.7~6.7	1.9~2.6	2.0~2.6	≤0.04	0.08~0.15	≤0.12	0.15	Bal.

Fig.1 Schematic diagram of LSP setup

Table 2 Experimental parameters of LSP

Process number	Thickness/ mm	Laser power density/GW·cm⁻²	Pulse width/ns	Continued LSP impacts at single spot	Spot size/mm	Confining layer thickness/mm	Absorbing layer thickness (3M aluminum foil)/mm
Process-1	0.33	3.78	7.32	1 time (LSP-1)	Φ3	4 (K9 glass)	0.1
Process-2	5	12.5	15	1~8 time (LSP-1~LSP-8)	4×4	1~2 (water)	0.12

with corrosive time of 10 s. Micro-hardnesses were measured by a HXD-1000TMC LCD Vickers indenter with a load of 2000 N and a dwell time of 5 s. The measurement spacing was 0.15 mm between successive points.

2 Results and Discussion

2.1 Rear free surface velocity measurements in 0.33 mm thick samples

Fig.2 shows the rear free surface velocity profiles recorded in Al7050 with 0.33 mm thickness. LSP shock breakout induces a steep acceleration of the rear free surface velocity. The measured profile of the rear free surface velocity shows a deceleration due to the reflection of the unloading wave from the rear free surface. At about 0.063 μs, an elastic precursor wave is generated. It indicates that the propagation of the elastic wave reaches the rear free surface at this time. And the rear free surface velocity is about 121 m/s. At 0.0761 μs, the rear free surface velocity reaches the first peak velocity of about 673.6 m/s. At 0.0882 μs, the rear free surface velocity reaches the first minimum velocity of about 378.4 m/s. It implies that spall damage at some distance beneath the rear free surface is initiated and induces a stress relaxation of the local tensile stresses (negative pressure). Then the compressive wave propagates from the spall plane to the rear free surface and produces a reacceleration called the spall pulse[22]. Thereafter, wave reverberates between the spall plane and the rear free surface, which produces damping oscillations. The velocity pullback Δu is from the peak velocity to the beginning of the spall pulse (first minimum velocity). According to an acoustic approximation and a roughness description of spall failure, the velocity pullback Δu is the maximum tensile stress induced by spall plane. The maximum tensile stress is referred to as the spall strength σ_R[17]:

$$\sigma_R = \rho_0 c_0 \Delta u / 2 \qquad (1)$$

where, ρ_0 is the initial material density of 2700 kg/m³. c_0 is the bulk sound speed of 5386 m/s[23]. Therefore, the spall strength of Al7050 with 0.33 mm thickness is 2.15 GPa.

The corresponding strain rate $\dot{\varepsilon}$ can be estimated as:

$$\dot{\varepsilon} = -\Delta u / 2c_0 \Delta t_1 \qquad (2)$$

where, $\Delta u / \Delta t_1$ is the mean slope of the deceleration Δu before the spall pulse. In the present LSP, the measured strain rate is about $2.3 \times 10^6 \, s^{-1}$.

The spall plate thickness h can be calculated as:

$$h = c_0 \cdot \Delta t_2 \qquad (3)$$

where, $\Delta t_2 = 0.0177 \, \mu s$ which is the time of going and back inside the target. Therefore, spall thickness is about 95.3 μm.

2.2 Observations of the spall crater in 0.33 mm thick samples

Fig.3 shows the fracture morphology of the spall crater of Al7050 with 0.33 mm thickness. It is evident that the spall is formed by the one layer lifting out, as shown in Fig.3a.The spall is in the form of a surface crater, as shown in Fig.3b. Surface crater is not circular spall, which may be attributed to laser

beam profile with spatial Gaussian distribution. Crack lines can be seen on the surrounding of crater. Fig.3c and Fig.3d are the higher magnifications of ellipse A and ellipse B in Fig.3b, respectively. The fracture surface consists of typical dimples and smooth surface. The dimples result from the nucleation, growth and coalescence of spherical voids under the tensile stress. The similar result has been reported and the strain rate is $0.8 \times 10^6 \, s^{-1}$ [23]. The detailed view in Fig.3d shows that the sizes of these voids at coalescence range from less than 1 μm to a few μm. The nucleation and the growth of straight cracks lead to smooth fracture surface, as shown in Fig.3c, which indicates a brittle behavior. The similar results have been researched in Ref. [24]. Therefore, the mixture ruptures behavior of Al7050 with 0.33 mm thickness is generated with the ductile behavior and the brittle behavior. The similar results have been reported in Ref. [16].

2.3 Spall detections with nondestructive testing in 5 mm thick samples

Fig.4 presents the images of C-scan of Al7050 with 5 mm thickness. No spall is observed in the shocked region after continued LSP-1~LSP-4, as shown in Fig.4a. However, the spall is observed in the shock region after continued LSP-5~LSP-8. Therefore, continued LSP-5 is the spall threshold of Al7050 with 5 mm thickness. The spall sizes increase with multiple LSP impact times. The spall sizes are 0.671 mm for continued LSP-5, 1.794 mm for continued LSP-6, 1.843 mm for continued LSP-7 and 1.555 mm for continued LSP-8. Fig.4b presents the spall thickness from the rear free surface after continued LSP-7. The spall thickness is 377 μm after continued LSP-7.

According to the criterion of the spall damage, the position of the spall in a thick metal is farther away from rear free surface than that in a thin metal. Therefore, the ejection of the spalled layers is generated in 0.33 mm thick Al7050 with LSP, as shown in Fig.3. However, the spall without ejection is formed in 5 mm thick Al7050 with continued multiple LSP, as shown in Fig.4.
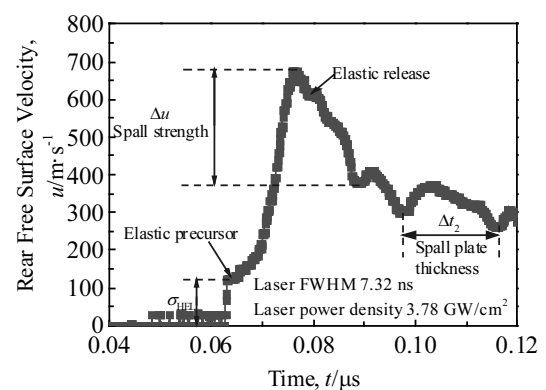

Fig.2   Rear free surface velocity profiles recorded in Al7050 with 0.33 mm thickness
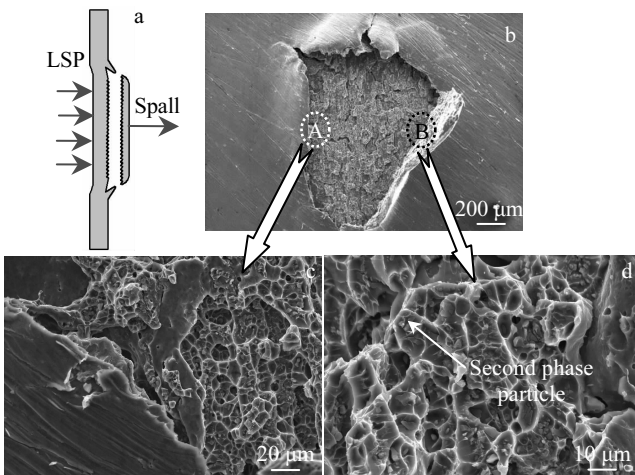
Fig.3 Schematic diagram of the spalled layer ejection (a) and fracture morphology of the spall crater of Al7050 with 0.33 mm thickness (b); magnified ellipse A (c) and ellipse B (d) in Fig.3b

2.4 Cross-sectional spall fracture characteristics in 5 mm thick samples

Fig.5 shows the cross-sectional spall fracture morphologies of Al7050 with 5 mm thickness near rear free surface. The inset in Fig.5a is the schematic of rectangle-like samples. The spall region (blue shaded) in the examined cross-section (light shaded) is normal to shock loading directions (arrows' indicating), far away from the lateral boundary of the sample. The marked square is the exact location of the regions illustrated in Fig.5a. Continuous cracks/spalls are observed in Fig.5. The thickness of the separated layer is uniform along

the spall plane. The spall thicknesses are measured to be 364 μm for continued LSP-5, 343 μm for continued LSP-6, 359 μm for continued LSP-7, 360 μm for continued LSP-8. The spall thickness measured by OM images in Fig.5c is nearly consistent with the spall thickness measured by C-scan in Fig.4b after LSP-7.

SEM characterization of the cross-sectional spall fracture morphology could be performed to gain insight into the physical nature of the damage evolution in Al7050 with 5 mm thickness. Fig.6 shows SEM images of the spall of Al7050 with 5 mm thickness. The SEM microstructure displays the typical features of ductile behavior. The spall damage consists of the nucleation,
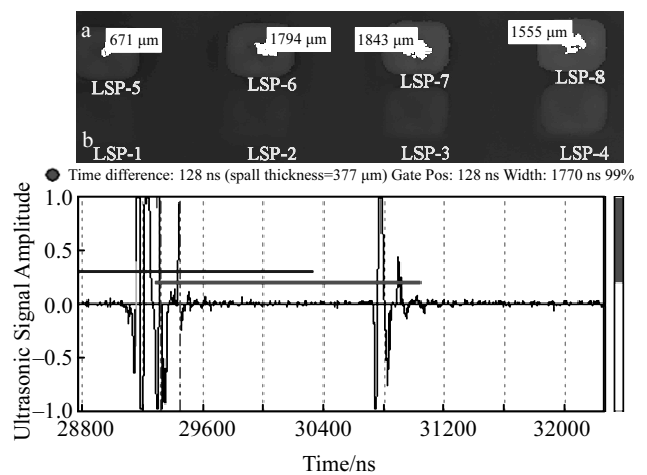

Fig.4 Images of C-scan of Al7050 with 5 mm thickness: (a) spall sizes and (b) spall thickness after continued LSP-7
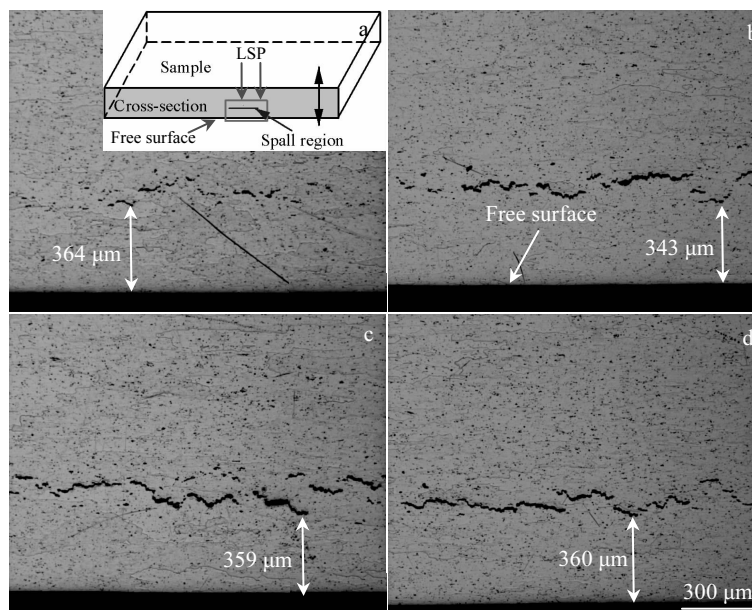

Fig.5 Cross-sectional spall fracture morphologies of Al7050 with 5 mm thickness near rear free surface: (a) continued LSP-5, (b) continued LSP-6, (c) continued LSP-7, and (d) continued LSP-8 (the inset in Fig.5a is the schematic of rectangle-like sample)
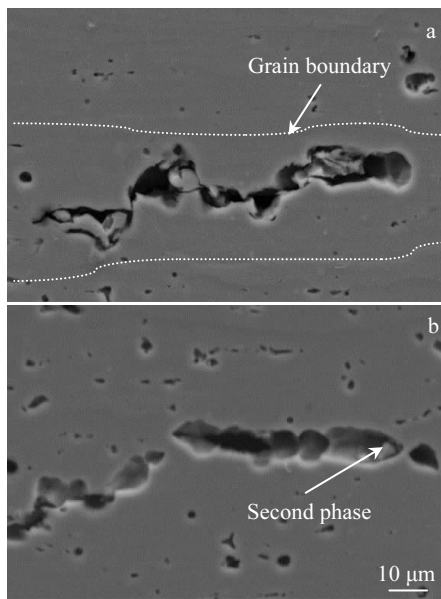
Fig.6   SEM images of the spall of Al7050 with 5 mm thickness:
(a) transgranular failure and (b) nucleation at the second phase

Fig.7   Surface microhardness of Al7050 with continued LSP-5 at the
cross section (a) and the edge of the dent (b)

growth, and coalescence of spherical voids. The voids are distributed in a narrow and concentrated range, and their coalescences are a simple process of direct contact of the grown voids. The damage microstructure of the spall also reveals the ductile transgranular failure, as shown in Fig.6a. The similar result has been reported in laser-induced spall of aluminum and aluminum alloys[20]. The most voids or cracks are nucleated at the second phase particles, as shown in Fig.6b. The sizes of these voids at coalescence range from 1 μm to a few μm.

The void growth and coalescence are a process of energy dissipation, which is related to the damage distribution of the voids. For Al7050, the damage distribution of the voids is narrow and centralized. Therefore, the coalescence process leads to low energy dissipation, which indicates that the spall strength of Al7050 is low. As a general rule, void nucleation results from the in-homogeneity in plastic deformation between the matrix and the inclusions. Thus void initiation sites are usually at the second phase particles. Under the combined effect of the dynamic tensile stress induced by LSP and the mean stress or stress-triaxiality ratio, the voids grow, interact with each other and form the coalescence. It eventually leads to the overall observed spall.

2.5   Microhardness at the cross section

Fig.7 shows microhardness of Al7050 with continued LSP-5. Microhardness (HV) of as-received material is about 1135 MPa by the analysis of cross-sectional microhardness, as shown in Fig.7a. However, microhardnesses of Al7050 with continued LSP-5 increase to about 1180 MPa. It may be attributed to the cold working hardening layer, high density dislocations and nanocrystals in the surface layer induced by LSP. The cross-sectional microhardness after continued multiple LSP gradually
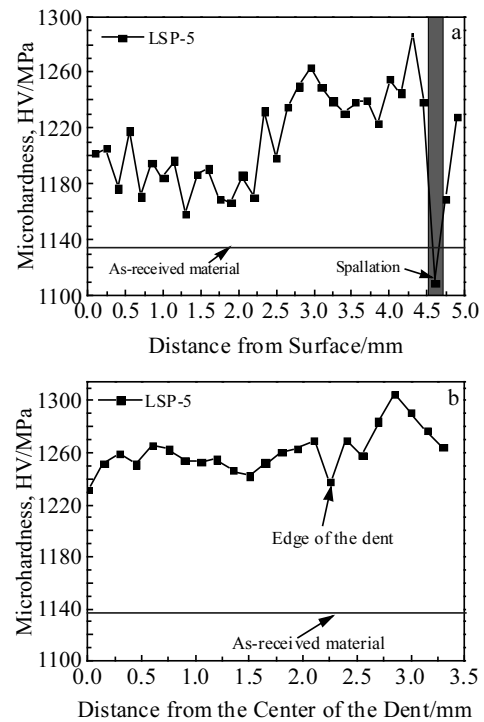
decreases with the increment of the distance from the surface. Similar results have been reported about TC11 alloy[25] and TC17 alloy[26]. These results may be ascribed to attenuation of the peak pressure of laser shock wave in the target. However, work soft and spall are generated near rear free surface, and microhardness falls to about 1109 MPa, which may be ascribed to high amplitude and long duration of dynamic tensile stress induced by LSP. Surface microhardness gradually increases from the center of dent to the edge of dent in the shocked area of Al7050, as shown in Fig.7b. Great hardness of Al7050 with LSP can bring a good property of fatigue resistance and prevent the foreign object damage (FOD) to some extent.

3   Conclusions

1) The spall strength and LSP strain rate in 0.33 mm thick Al7050 with LSP are 2.15 GPa and 2.3×10^6 s^{-1}, respectively. The fracture morphology of spall crater in 0.33 mm thick Al7050 is the mixture ruptures of the ductile with typical dimples and the brittle with smooth fracture surfaces. Typical dimples are the nucleation, growth and coalescence of spherical voids. Smooth fracture surfaces are generated by the nucleation and the growth of straight cracks.

2) Continued LSP-5 is the spall threshold in 5 mm thick Al7050. The plane spall sizes are 0.671 mm for continued LSP-5, 1.794 mm for continued LSP-6, and 1.843 mm for continued LSP-7 and 1.555 mm for continued LSP-8. The cross-sectional spall thicknesses of 5 mm thick Al7050 are

364 μm for continued LSP-5, 343 μm for continued LSP-6, 359 μm for continued LSP-7, 360 μm for continued LSP-8.

3) The cross-sectional spall fracture morphology shows that the most voids or cracks are nucleated at the second phase particles. Ductile transgranular failure forms. The micro-hardness of 5 mm thick Al7050 with continued LSP-5 increases from about 1135 MPa of as-received material to about 1180 MPa in the surface layer. However, work softing and spall are generated near rear free surface and micro-hardness decreases to about 1109 MPa.

References

1 Bergant Z, Trdan U, Grum J. *International Journal of Fatigue*[J], 2016, 87: 444

2 Lin B, Lupton C, Spanrad S *et al. International Journal of Fatigue*[J], 2014, 59: 23

3 Zhang Y K, Lu J Z, Ren X D *et al. Materials and Design*[J], 2009, 30(5): 1697

4 Gao Yukui. *Rare Metal Materials and Engineering*[J], 2016, 45(9): 2347 (in Chinese)

5 Peyre P, Fabbro R, Merrien P *et al. Materials Science and Engineering A*[J], 1996, 210(1-2): 102

6 Lescoute E, De Rességuier T, Chevalier J M *et al. Applied Physics Letters*[J], 2009, 95(21): 211 905

7 Mayer A E, Khishchenko K V, Levashov P R *et al. Journal of Applied Physics*[J], 2013, 113(19): 193 508

8 Fortov V E, Kostin V V, Eliezer S. *Journal of Applied Physics*[J], 1991, 70(8): 4524

9 Loison D, De Rességuier T, Dragon A *et al. Journal of Applied Physics*[J], 2012, 112(11): 113 520

10 Tollier L, Fabbro R. *Journal of Applied Physics*[J], 1998, 83(3): 1231

11 Wang Y, He H, Wang L *et al. Journal of Applied Physics*[J], 2006, 100: 325

12 Wang Y G, Qi M L, He H L *et al. Mechanics of Materials*[J], 2014, 69(1): 270

13 De Rességuier T, He H, Berterretche P. *International Journal of Impact Engineering*[J], 2005, 31(8): 945

14 Cottet F, Boustie M. *Journal of Applied Physics*[J], 1989, 66(9): 4067

15 Tyler C, Millett J C F, Bourne N K. *AIP Conference Proceedings*[J], 2006, 845(1): 674

16 Lescoute E, De Rességuier T, Chevalier J M *et al. Journal of Applied Physics*[J], 2010, 108(9): 093 510

17 De Rességuier T, Signor L, Dragon A *et al. Journal of Applied Physics*[J], 2007, 102(7): 073 535

18 Jarmakani H, Maddox B, Wei C T *et al. Acta Materialia*[J], 2010, 58(14): 4604

19 Wielewski E, Appleby-Thomas G J, Hazell P J *et al. Materials Science and Engineering A*[J], 2013, 578: 331

20 Dalton D A, Brewer J L, Bernstein A C *et al. Journal of Applied Physics*[J], 2008, 104(1): 013 526

21 Wu X Q, Duan Z P, Song H W *et al. Journal of Applied Physics*[J], 2011, 110: 1021

22 Kanel G I. *International Journal of Fracture*[J], 2010, 163(1-2): 173

23 Tollier L, Fabbro R, Bartnicki E. *Journal of Applied Physics*[J], 1998, 83: 1224

24 Cuq-Lelandais J P, Boustie M, Berthe L *et al. Journal of Physics D: Applied Physics*[J], 2009, 42(6): 65 402

25 Nie X F, He W F, Zang S L *et al. Surface and Coatings Technology*[J], 2014, 253: 68

26 Nie X F, He W F, Li Q P *et al. Journal of Laser Applications*[J], 2013, 25(4): 042 001

超高应变率激光冲击不同厚度 Al7050 合金的层裂研究

吴俊峰，邹世坤，车志刚，巩水利，曹子文

(中国航空制造技术研究院 高能束流加工技术重点实验室，北京 100024)

摘　要：分析不同工艺参数（工艺 1 和工艺 2）激光冲击不同厚度 Al7050 合金的层裂特性，研究 Al7050 合金的层裂机理和层裂阈值。采用光子多普勒测速（PDV）系统和扫描电镜（SEM），分析工艺 1 激光冲击 0.33 mm 厚 Al7050 合金的自由面质点速度和自由面层裂断口形貌。采用超声波无损检测、光学显微镜（OM）和扫描电镜（SEM），分析工艺 2 激光冲击 5 mm 厚 Al7050 合金的层裂大小、层裂厚度和层裂断口形貌。研究结果表明，基于 PDV 测试数据，获得激光冲击 0.33 mm 厚 Al7050 合金的层裂强度和激光冲击应变率。0.33 mm 厚 Al7050 合金的自由面断口形貌被详细分析。随着连续激光冲击次数增加，5 mm 厚 Al7050 合金的层裂尺寸增加，层裂厚度范围为 343 μm 到 364 μm。层裂机理为微空洞的韧性断裂和直裂纹的脆性断裂的混合断裂。单点连续 5 次激光冲击为 5 mm 厚 Al7050 合金的层裂阈值。与基体材料相比，单点连续 5 次激光冲击 5 mm 厚 Al7050 合金的表层显微硬度提高，而自由面附近的显微硬度降低。研究结果不仅为激光冲击强化铝合金的层裂行为研究提供重要见解，而且为激光冲击强化工业应用避免层裂提供基础研究。

关键词：Al7050 合金；激光冲击强化；层裂机理；层裂阈值；层裂断口形貌

作者简介：吴俊峰，男，1988 年生，博士生，中国航空制造技术研究院高能束流加工技术重点实验室，北京 100024，E-mail: wjf88813@163.com